Title

Mixed valence copper–sulfur clusters of highest nuclearity: a Cu 8 wheel and a Cu 16 nanoball

Journal

Chemical Communications, 53(23)

ISSN

1359-7345

Authors

Maji, Ram Chandra
Das, Partha Pratim
Bhandari, Anirban
et al.

Publication Date

2017-03-16

DOI

10.1039/c6cc08301c

Peer reviewed

Journal Name

COMMUNICATION

Mixed Valence Copper-Sulfur Clusters of High Nuclearity: A Cu_8 Wheel and a Cu_{16} Nanoball

Received 00th January 20xx,
Accepted 00th January 20xx

DOI: 10.1039/x0xx00000x

www.rsc.org/

Ram Chandra Maji,[a] Partha Pratim Das,[b] Anirban Bhandari,[a] Saikat Mishra,[a] Milan Maji,[a] Kamran B. Ghiassi,[c] Marilyn M. Olmstead[c] and Apurba K. Patra[a]*

Fully spin delocalized mixed valence copper-sulfur clusters, 1 and 2, supported by μ4-sulfido and NS^{thiol} donor ligands are synthesized and characterized. Wheel-shaped 1 consists of Cu_2S_2 units. The unprecedented nanoball 2 can be described as S@Cu4(tetrahedron)@O6(octahedron)@Cu12S12(cage) consisting of both Cu_2S_2 and $(\mu_4\text{-}S)Cu_4$ units. The Cu_2S_2 and $(\mu_4\text{-}S)Cu_4$ units resemble biological Cu_A and Cu_Z sites, respectively.

Sulfur complexes of transition metals,[1] particularly those of iron and copper[2] are ubiquitous in nature, acting as electron transfer agents, catalytic sites for biochemical reactions and for metal-storage and release. In addition to these biological roles, the synthetic high-nuclearity metal clusters are of current research interest owing to their use as nanomaterials, catalysts,[3] and single-molecule magnets.[4] The *bis*-cysteine-S bridged binuclear Cu_A site is a well-recognized electron transfer agent in biology, found in the enzymes cytochrome c oxidase (CcO)[5] and nitrous oxide reductase (N_2OR).[6] CcO catalytically reduces $O_2 \rightarrow H_2O$ during respiration while the latter (N_2OR) catalytically reduces $N_2O \rightarrow N_2$ during denitrification. Throughout the catalytic action, the Cu_A site shuttles between the fully spin delocalized mixed valence (MV), $Cu^{+1.5}$-$Cu^{+1.5}$ and its fully reduced Cu^{+1}-Cu^{+1} form. In addition to the Cu_A site, the enzyme N_2OR features a μ_4-sulfido bridged MV tetra-copper cluster, $[His_7(\mu\text{-}OH/H_2O?)(\mu_4\text{-}S)Cu^{II}Cu^{I}_3]$, known as the Cu_Z site. The Cu_A site reduces the MV Cu_Z to a fully reduced $(\mu_4\text{-}S)Cu^{I}_4$ cluster that acts as the catalytic site for N_2O reduction to N_2. Also, $Cu^{I}_mS^{thiol}_n$ clusters (m = 4, 6 and 8) are found in the copper metallothionein[7] proteins that function as storage, transport, metabolism and acquisition of Cu in biological systems.

The highest nuclearity Cu_mS_n cluster containing Cu^{I} ions is $[Cu^{I}_{136}S_{56}(SCH_2C_4H_3O)_{24}(dpppt)_{10}]$ (dpppt = 1,5-*bis*(diphenylphosphino)pentane).[8] In the absence of sulfur, but with stronger N and O donor ligands, the highest nuclearity cluster containing only Cu^{II} ions is $[Cu_{44}(\mu_8\text{-}Br)_2\text{-}(\mu_3\text{-}OH)_{36}(\mu\text{-}OH)_4(ntp)_{12}Br_8(OH_2)_{28}]Br_2 \bullet 81H_2O$ (ntp= nitrilotripropionic acid).[9] It has been shown that sulfur in the presence of additional N donors can stabilize mono-,[10] bi-,[11] spin localized MV[12] and, rarely, spin delocalized MV[13] complexes. The only known spin delocalized MV Cu_A site model supported by an aliphatic thiol containing a NS donor ligand is $[\{(L^{iPrdaco}S)Cu\}_2]O_3SCF_3$.[13a] With the use of NS donor aromatic thiol ligands, examples so far are: a mono-thiolato bridged binuclear species,[13b] $\{N_6Cu_2S\}^{2+}$, and a thiolato-bridged cluster, $\{N_6Cu_6S_6\}^{2+}$.[13c] Diverse examples of Cu_mS_n complexes[14] are known but the (i) MV variety (spin localised or delocalised) that contain both thiolato- and sulfido-sulfur donor, and (ii) a complex (regardless of Cu valence states) that contains both Cu_2S_2 and $(\mu_4\text{-}S)Cu_4$ units are unknown, although model complexes possessing discrete $(\mu_4\text{-}S)Cu^{MV}_4$, $(\mu_4\text{-}S)Cu^{I}_4$ and $(\mu_3\text{-}S)Cu^{MV}_3$ cores relevant to the Cu_Z site of N_2OR are documented.[15]

Herein, we report two fully spin delocalized MV copper clusters, $[(L1)_8Cu^{I}_6Cu^{II}_2](ClO_4)_2 \bullet DMF \bullet 0.5CH_3OH$ (**1**) and $[(L2)_{12}Cu^{I}_5Cu^{II}_{11}(\mu_4\text{-}S)(\mu_4\text{-}O)_6](ClO_4) \bullet 4H_2O$ (**2**) with supporting NS^{thiol} and sulfido-S (generated in-situ from C-S bond cleavage) donor ligands. No aromatic or aliphatic thiol-S donor MV copper complexes of higher nuclearity than **1** and **2** have been reported. The MV **2** is unique since both Cu_2S_2 and $(\mu_4\text{-}S)Cu_4$ units are present.

Condensation of thiophene-2-carboxaldehyde with 2-aminobenzenethiol or cysteinamine under refluxing conditions in dry CH_3OH produces the corresponding disulfide ligands, $L1^{S\text{-}S}$ and $L2^{S\text{-}S}$. When solid $[Cu^{I}(CH_3CN)_4]ClO_4$ (g, mmol) is added to a light yellow solution of $L1^{S\text{-}S}$ (g, mmol) in CH_3OH under N_2 a dark reddish purple color is generated and after XX hours a purple solid precipitates out (Scheme 1). Ether diffusion to a DMF solution of the solid yields X-ray quality crystals of **1** in high yield (76% w.r.t Cu). Following a similar synthetic procedure but with the $L2^{S\text{-}S}$ ligand results in precipitation of a yellow solid. Upon dissolution in DMF, the yellow solid changes

[a] *Department of Chemistry, National Institute of Technology Durgapur, Durgapur 713 209, west Bengal, India.*
[b] *Department of Chemistry, Indian Institute of Technology Kanpur, Kanpur 208 016, Uttar Pradesh, India*
[c] *Department of Chemistry, University of California Davis, CA 95616, USA.*

Electronic Supplementary Information (ESI) available: Synthesis and characterisation of ligands and complexes, Full molecular view of **1** and **2**, Bond distances and angles table, crystallographic data and structure refinement parameters of **1** and **2**.

to reddish brown in the presence of O_2. The yellow color persists in the absence of O_2, even if H_2O or CH_3OH is added to DMF, and yields dark brown blocks of **2** (yield w.r.t Cu = 80%) as a major product. A green side product is insoluble in all common organic solvents.

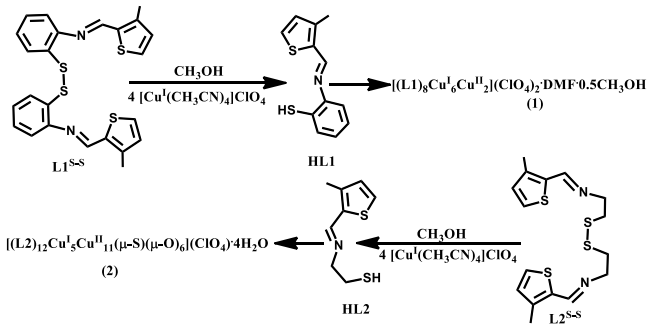

Scheme 1. ChemDraw depiction of ligands and synthesis of **1** & **2**

The X-ray structure of **1** consists of eight Cu ions in a crown conformation and eight μ_3-S bridging atoms in a square anti-prismatic array, leading to a $\{Cu_8S_8\}$ wheel structure as shown in Figure 1. The copper ions adopt a distorted tetrahedral coordination geometry with NS donor atoms of a ligand and two other μ_3-S donors of two adjacent ligands. External to the wheel, thiophene-S to Cu distances range between 3.142 Å - 3.252 Å. As a whole, the four $\{Cu_2(NS)_2\}$ units found in the wheel are linked to each other *via* their thiolato-S. Each of the eight "spokes" of the wheel is spanned by a ligand. The Cu-S-Cu angles consist of one wide 121.6(9)°(ave) angle and two more acute angles at 66.6(5)° (ave). The average Cu-S, Cu-Cu and Cu-N distances of 2.335(3) Å, 2.5812(17) Å and 2.042(10) Å, respectively, are very close to the corresponding values for the Cu_A site that has Cu-S ~ 2.32 Å (ave), Cu–Cu ~2.51 Å, Cu-N ~2.00 Å (ave) and Cu–S–Cu ~63° (ESI).[2] The acute Cu–S–Cu bridging angle promotes a strong dπ-pπ Cu–S covalent character, and the short Cu-Cu distances reveal metal-metal interactions. The bond distances and angles of each Cu_2S_2 unit of **1** closely resemble one another and resemble a reported spin delocalised MV wheel shaped cluster, $[\{Cu^I_2Cu^{II}(NguaS)_3\}_2](PF_6)_2$[13c] as well as those of the Cu_A site (ESI). These features mimic the valence delocalization and MV character of the Cu_A site. The structure of **1** is in keeping with the MV $\{Cu^{II}_2Cu^I_6\}^{2+}$ core. The diameter of the Cu_8 wheel (farthest Cu–Cu distance) of 5.836 Å is smaller than nanoparticle size, therefore, the Cu_8S_8 framework of **1** may be considered as a nanowheel. The isotopic distribution pattern of a peak at *m/z* = 1183.200 in ESI mass spectrum of **1** is consistent with $[(L1)_8Cu_8]^{2+}$ formulation (ESI).

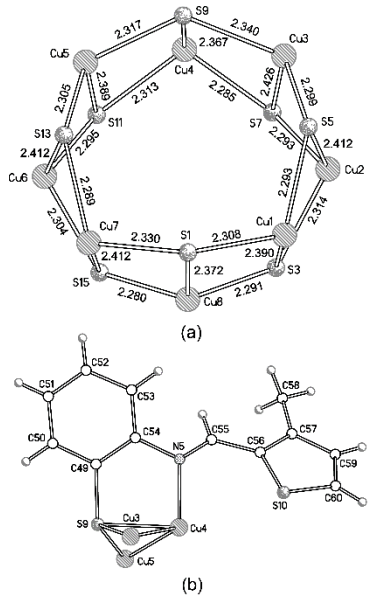

Figure 1. Structure of the cationic $\{Cu_8S_8\}$ part of **1** (a) and the ligand (L1) that bridges a spoke of the wheel (b).

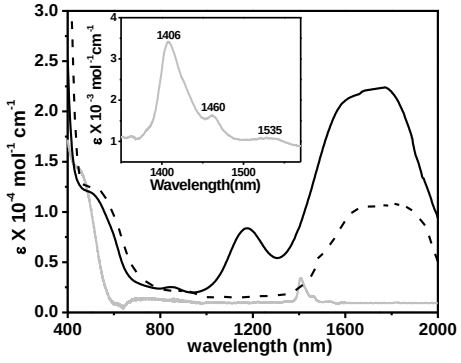

Figure 2. Vis-NIR spectrum of **1** in CH_3CN (black), coulometrically reduced $\mathbf{1}^{Red}$ (dash) and **2** (gray). Inset: enlarged, lower energy absorptions of **2**.

The electronic absorption spectra (UV-Vis and Vis-NIR) of **1** feature bands at λ_{max}(nm), (ε in $M^{-1}cm^{-1}$) = 269 (77250), 314 (88875), 350 (sh, 63320), 500 (11820), 850(2510), 1175(8310) and centered at 1700 (21930), Figure 2. Based on the high ε values and solvent independency (expected for a valence delocalized MV valence, class III system[16]), the lower energy bands at 1700 nm and 1175 nm are assigned to the inter valence charge transfer transitions (IVCT) or $\Psi \rightarrow \Psi^*$ transition. The lowest energy band of **1** is substantially red-shifted compared to the Cu_A site but is comparable to those of the reported model complexes including $[\{(L^{iPrdaco}S)Cu\}_2]O_3SCF_3$.[17] Other transitions at 850 nm and 500 nm are likely due to the thiol-$S^- \rightarrow Cu^{II}$ charge transfer transitions (LMCT), while the 350 nm and 269 nm bands are due to the ligand n-π* and π–π* transitions, respectively.

The short Cu–Cu distance and highly covalent Cu-S_{cys} bonding in the MV Cu_A site ($Cu^{+1.5}$-$Cu^{+1.5}$ form), greatly lowers the reorganization energy for $Cu^{+1.5}$-$Cu^{+1.5}$ → Cu^{+1}-Cu^{+1} reduction, and ensures rapid electron transfer during catalytic turnover of the enzymes. A mean reduction potential of

+0.039 V *vs* SCE is reported for the Cu_A site of CcO.[18] The similar geometry of the Cu_2S_2 units of **1** to that of the Cu_A site tempted us to investigate its redox properties. The cyclic voltammogram (CV) measured in CH_3CN features one reversible redox response at $E_{1/2}$ = -0.029 V (ΔE_p = 58 mV, i_{pa}/i_{pc} ≈1) and a quasi-reversible response at $E_{1/2}$ = -0.326 V (ΔE_p = 91 mV, i_{pa}/i_{pc} <<1) corresponds to the $Cu^{II}_2Cu^{I}_6/Cu^{II}Cu^{I}_7$ and $Cu^{II}Cu^{I}_7/Cu^{I}_8$ couples, respectively (Figure 3, inset). To check the reversibility of $Cu^{II}_2Cu^{I}_6/Cu^{II}Cu^{I}_7$ couple observed at $E_{1/2}$ = -0.029 V, variable scan rates (0.02 Vs^{-1} to 1 Vs^{-1}) CV were measured. These results indicate

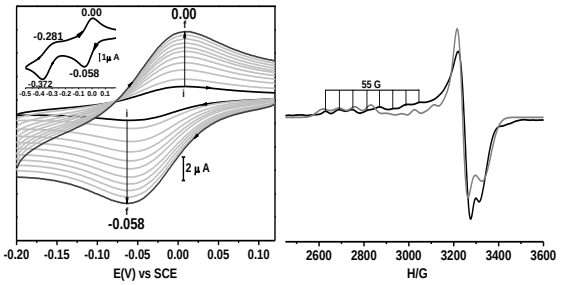

Figure 3, Left: CV traces of **1** in CH_3CN with Pt and SCE as working and reference electrode respectively at various scan rates, 0.05, 0.1, 0.2, 0.3, 0.4, 0.5, 0.6, 0.7, 0.8, 0.9, 1.0 Vs^{-1} (i→f, sequential traces from 0.05→1.0 Vs^{-1}). Inset: CV trace, showing both cathodic responses; **Right**: X-band EPR spectrum of **2** in CH_3CN/toluene at 100 K (black) and simulated spectrum (gray), microwave frequency and power 9.545 GHz and 0.189 mW.

complete retention of ΔE_p (58 mV), E_{pc}, E_{pa} and i_{pa}/i_{pc} ratio ≈ 1 validating **1**→**1**^{red} reduction as fully reversible (Figure 3). Constant potential electrolysis at -0.2 V generates **1**^{red} that exhibits a $\Psi \rightarrow \Psi^*$ transition at 1775 nm, indicative of the valence delocalized, class III(need ref) behavior of **1**^{red} (Figure 2). Upon reduction, **1**→**1**^{Red}, the noticeable differences in the electronic absorption spectrum observed are: [λ_{max} (nm)(ε in $M^{-1}cm^{-1}$) = 269 (78790), 314(90695), 350 (sh, 63320), 520 (12390), 850(2240), and centered at 1775 (10700)], a sharp decrease of ε at 1700 nm and the disappearance of the 1175 nm band (Figure 2 and ESI). This electrochemically generated CH_3CN solution at 120 K exhibits an isotropic EPR signal at g = 2.037 corroborating one electron reduction of **1** to a $Cu^{II}Cu^{I}_7$ core.

To check whether the self-assembly yields a similar octanuclear cluster to **1**, and following a similar synthetic procedure but with a flexible aliphatic thiol ligand $L2^-$ instead of $L1^-$, we have synthesized **2**. Dark brown block shaped crystals were characterized by single crystal X-ray diffraction studies using synchrotron radiation at 100 K. Several other datasets were collected; however, the same disorder of the structure was found. The structure determination revealed a convex $\{Cu_{12}S_{12}\}$ sphere of a somewhat distorted truncated octahedron (an Archimedean polygon with 24 vertices, eight hexagons and six squares associated with 3-fold symmetry) with twelve copper and twelve thiolato-S atoms positioned on 24 vertices as shown in Figure 4a. The diameter of the $\{Cu_{12}S_{12}\}$ sphere is 7.86 Å (distance of two farthest Cu atoms). If the capping thiophene rings (see Figure 4b) are included, the farthest $CH_3\cdots CH_3$ distance is 19.44 Å, thus well within nano-particle size. The interior describes an unprecedented molecular arrangement of a tetrahedral Cu_4S moiety, interdigitated with an O_6 octahedron.

Two types of Cu_2S_2 structural units exist in **2**: those of six Cu_2S_2 units present in the $\{Cu_{12}S_{12}\}$ outermost region of the sphere and those of a total of twelve Cu_2S_2 units formed where one of the Cu's of the Cu_4 tetrahedron is common (Figure 5). The Cu_2S_2 squares of the first type have alternate long and short Cu-S distances in the range 2.831(7) Å - 2.857(7) Å and 2.250(6) Å - 2.373(6) Å with a Cu–Cu distance in the range 3.086(5)-3.136(5) Å and Cu-S-Cu angles in the range 73.50(20)°-75.70(18)°. The Cu-Cu distance and the Cu-S-Cu angle resemble the DFT-optimized π_u ground

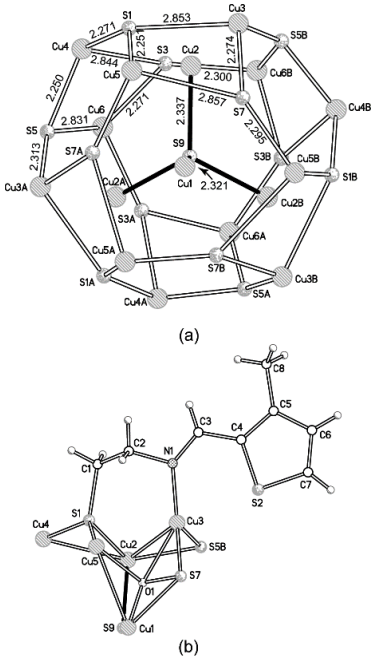

Figure 4. (a) A view down the *c* direction of the copper and sulfur atoms of the encaged (μ_4-S)Cu_4 tetrahedron and the $\{Cu_{12}S_{12}\}$ outer cage in the structure of **2**. Atoms labeled A and B are generated by the 3-fold crystallographic site symmetry: A = 1-y, x-y, z and B = 1-x+y, 1-x, z. Distances are given in Å and the standard uncertainties range from 0.004 to 0.007 Å. Bonds to Cu1 and Cu2 are omitted in order to show only the convex surface. (b) A selection of the atoms in the structure showing the capping by L2 and including those between the outer cage and the encaged atoms.

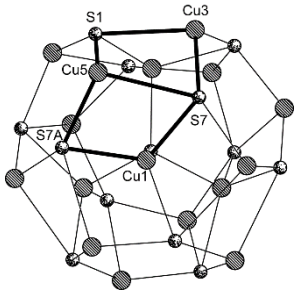

Figure 5. Heavy lines depict the two different kinds of Cu_2S_2 units that occur in the set $\{Cu_{12}S_{12}(Cu_4S)\}$. The atom labelled Cu1 is the unique atom that resides on the 3-fold axis of the central (Cu_4S). The remaining labelled atoms reside in the convex surface.

state of the Cu_A site.[19] For the second type of Cu_2S_2, there are three short Cu–S bonds in the range 2.271(7) Å - 2.377(6) Å and one long Cu–S bond (this is the shared edge shown in Figure 5) in the range 2.831(7) Å - 2.857(7) Å with Cu–Cu

distances in the range 2.779(4) Å – 2.847(4)Å. Two Cu-S-Cu angles, one ranging from 63.95(20)° to 65.33(18)° and other 73.41(19)°to 75.62(18)°, correspond respectively to σ_u* and π_u ground states of the Cu_A site.[19] No examples are reported where, in the same Cu_2S_2 unit, the two Cu–S–Cu angles differ to such an extent. In the structure of **2** the angles can be attributed to the overall structural requirements.

The interior (μ_4-S)Cu_4 moiety features Cu-S distances in the range 2.321(9)-2.337(4) Å and nearly perfect tetrahedral geometry about the central S atom [tau(4) – 0.99, see ESI]. In contrast, the (μ_4-S)Cu_4 moiety of the Cu_Z site adopts a distorted square pyramidal geometry with sulfido-S at the apex of a Cu_4 plane. Among the four Cu-O bonds observed for each μ_4-O, one Cu–O distance is significantly shorter[20] (in the range 1.62(3) Å -1.668(12) Å) than the normal Cu–O distance reported, possibly due to the geometry restraint imposed by the $\{Cu_{12}S_{12}\}$ sphere or, more likely, due to the structural disorder. Interestingly, in the Cu_Z site a Cu bridged O atom (H_2O/OH^-?) is also structurally evident. It is replaced when N_2O binds and gets reduced to N_2 during catalytic turn-over.[21]

The positive ion ESI mass spectrum of **2** displays a prominent peak at *m/z* = 1680.05, corresponding to the molecular ion, $[\{(L2)_{12}Cu^{I}_{5}Cu^{II}_{11}(\mu_4\text{-}S)(\mu_4\text{-}O)_6\} + 3H]^{2+}$. The theoretical isotopic pattern matches well to the experimentally observed (see ESI) spectrum. The Vis-NIR spectrum (Figure 2, gray trace) displays the $\Psi \rightarrow \Psi^*$ transition at 1406 nm with two weak shoulders at 1460 nm and 1535 nm. The model $[\{(L^{iPrdaco}S)Cu\}_2]O_3SCF_3$ displays this transition at 1466 nm. The absorptions at ~700 nm and 440 nm are due to the thiolato-S^- to Cu^{II} charge transfer transition. The EPR spectrum of **2**, measured in CH_3CN/toluene glass at 120 K, features seven line hyperfine splitting of the $g_{||}$ band with an average $A_{||}$ value of 55 G (Figure 3, right), in keeping with the valence delocalized MV character of **2**.[13a] Simulation, considering interaction of one unpaired spin with two Cu nuclei, revealed g_1 = 2.480, g_2 = 2.088, g_3 = 2.028, A_1^{Cu} = 85 G and $A_2^{Cu} = A_3^{Cu}$ = 8 G. The magnetic moment, μ_{eff}, value of 2.43μ_B (296.90 K) and 0.89μ_B (3.48 K) of **1** (μ_{eff}/cluster: 3.43 μ_B at 296.90 K and 0.63 μ_B at 3.48 K) and of 3.07μ_B (296.97 K) and 0.69μ_B (3.82 K) of **2** (μ_{eff}/cluster: 10.18 μ_B at 296.97 K and 2.30 μ_B at 3.82 K), measured at 500 Oe external magnetic field, represents antiferromagnetic coupling (supports valence delocalisation) of the unpaired spins of Cu^{II} ions in $\{Cu^{II}_2Cu^{I}_6\}$ in **1** and in the $\{Cu^{II}_{11}Cu^{I}_5\}$ core of **2**.

Conclusions

In conclusion, we have synthesized high nuclearity, spin-delocalized MV copper-sulfur complexes: one with an aromatic thiol (**1**) and other with an aliphatic thiol containing NS^{thiol} plus sulfido, S^{2-} ligand (**2**). Though bigger in size, complex **1**, associated with Cu_2S_2 units and **2**, associated with Cu_2S_2 and μ_4-SCu_4 units reproduce many of the structural and spectroscopic properties of biological Cu_A and Cu_Z sites. Spin-delocalized MV **2** is unique where both Cu_2S_2 and μ_4-SCu_4 units are present (adjacent Cu_A and Cu_Z sites are evident in N_2OR).

Notes and references

$ We acknowledge SERB (project # EMR/2014/001059); the AvH Foundation, Germany (equipment donation grant) and UGC (fellowship to R.C.M) for financial support. We thank the Advanced Light Source, Lawrence Berkeley Lab for use of beam line 11.3.1 for X-ray data collection. The Advanced Light Source is supported by the Director, Office of Science, Office of Basic Energy Sciences of the U. S. Department of Energy under Contract No. DE-AC02-05CH11231. We sincerely thank Prof. R. Mukherjee, IIT Kanpur for providing various instrumental facilities, and Dr. Shilpam Sharma, Material Science Group, IGCAR, Kalpakkam for preliminary magnetic measurements.

1 E. I. Stiefel, K. Matsumoto, Eds. *Transition Metal Sulfur Chemistry*, American Chemical Society; Washington DC, 1996.
2 (a) E. I. Solomon, D. E. Heppner, E. M. Jhonston, J. W. Ginsbach, J. Cirera, M. Qayyum, M. T. Kieber-Emmons, C. H. Kjaergaard, R. G. Hadt, L. Tian, *Chem. Rev*. 2014, ***114***, 3659; (b) J. Liu, S. Chakraborty, P. Hosseinzadeh, Y. Yu, S. Tian, I. Petrik, A. Bhagi, Y. Lu, *Chem. Rev.* 2014, ***114***, 4366.
3 M. B. Gawande, A. Goswami, F-X. Felpin, T. Asefa, X. Huang, R. Silva, X. Zou, R. Zboril, R. S. Varma, *Chem. Rev.* 2016, ***116***, 3722.
4 H. L. C. Feltham, S. Brooker, *Coord. Chem. Rev.* 2014, ***276***, 1.
5 S. Iwata, C. Ostermeier, B. Ludwig, H. Michel, *Nature*, 1995, ***376***, 660.
6 K. Brown, M. Tegon, M. Prudencio, A. S. Pereira, S. Besson, J. J. G. Moura, I. Moura, M. Tegoni, C. Cambillau, *Nat. Struct. Biol.* 2000, **7**, 191.
7 V. Calderone, B. Dolderer, H. J. Hartmann, H. Echner, C. Luchinat, C. D. Bianco, S. Mangani, U. Weser, *Proc. Natl. Acad. Sci. USA*, 2005, ***102***, 51.
8 M-L. Fu, I. Issac, D. Fenske, O. Fuhr, *Angew. Chem. Int. Ed*. 2010, ***49***, 6899.
9 M. Murugesu, R. Clérac, C. E. Anson, A. K. Powell, *Inorg. Chem.* 2004, ***43***, 7269.
10 (a) Y. Lee, A. A. N. Sarjeant, K. D. Karlin, *Chem. Commun.,* 2006, 621; (b) A. J. Adwards, R. S. Dhayal, P. Liao, J. Liao, M. Chiang, R. O. Piltz, S. Kahlal, J. Saillard, C. W. Liu, *Angew. Chem.* 2014, ***126***, 7342; (c) S. Schneider, J. A. S. Roberts, M. R. Salata, T. J. Marks, *Angew. Chem. Int. Ed.* 2006, ***45***, 1733.
11 (a) R. P. Houser, J. A. Halfen, V. G. Young Jr., N. J. Blackburn, W. B. Tolman, *J. Am. Chem. Soc.* 1995, ***117***, 10745; (b) A. Neuba, R. Haase, W. Meyer-Klaucke, U. Flörke, G. Henkel, *Angew. Chem. Int. Ed.* 2012, ***51***, 1714; (c) Y. Ueno,; Y. Tachi, S. Itoh, *J. Am. Chem. Soc.* 2002, ***124***, 12428.
12 (a) R. P. Houser, W. B. Tolman, *Inorg. Chem*. 1995, ***34***, 1632; (b) S. Roy, S. Javed, M. M. Olmstead, A. K. Patra, *Dalton Transactions*, 2011, **40**, 12866.
13 (a) R. P. Houser, V. G. Young Jr., W. B. Tolman, *J. Am. Chem. Soc.* 1996, ***118***, 2101; (b) S. Torelli, M. Orio, J. Pécaut, H. Jamet, L. L. Pape, S. Ménage, *Angew. Chem. Int. Ed.* 2010, ***49***, 8249; (c) A. Neuba,; U. Flörke, W. Meyer-Klaucke, M. Salomone-Stagni, E. Bill, E. Bothe, P. Höfer, G. Henkel, *Angew. Chem. Int. Ed.* 2011, ***50***, 4503.
14 O. Fuhr, S. Dehnen, D. Fenske, *Chem. Soc. Rev.* 2013, ***42***, 1871.
15 (a) B. J. Johnson, S. V. Lindeman, N. P. Mankad, *Inorg. Chem.* 2014**,** ***53***, 10611; (b) G. N. D. Francesco, A. Gaillard, I. Ghiviriga, K. A. Abboud, L. J. Murray, *Inorg. Chem.* 2014, ***53***, 4647; (c) B. J. Johnson, W. E. Antholine, S. V. Lindeman, M. J. Graham, N. P. Mankad, *J. Am. Chem. Soc.* 2016, ***138***, 13107.
16 K. D. Demadis, C. M. Hartshorn, T. J. Meyer, *Chem. Rev.* 2001, ***101***, 2655.
17 Soluble Cu_A of *P. denitrificans* [in nm (ε)]: 363 (1200), 480 (3000), 532 (3000), 808 (1600); Cu_Z of *P. nautica*: 356 (3295),

500 (930), 700 (1455), 638 (3470), 1000 (1760); $[(L^{iProdacoS}Cu)_2]^{2+}$ in CH_3OH[13a]: 358 (2700), 602 (800), 786 (sh), 1466 (1200)

18 a) H. Wang, D. F. Blair, W. R. Ellis Jr, H. B. Gray, S. I. Chan, *Biochemistry* **1986**, *25*, 167-171.

19 S. I. Gorelsky, X. Xie, Y. Chen,; J. A. Fee, E. I. Solomon, *J. Am. Chem. Soc*. **2006**, *128*, 16452-16453.

20 G. Lanzani, K. Laasonen,; *Surface Science*, **2008**, *602*, 321-344.

21 P. Chen, S. I. Gorelsky, S. Ghosh, E. I. Solomon, *Angew. Chem. Int. Ed.* **2004**, *43*, 4132-4140.